

Imaging of acute pulmonary embolism: an update

Alastair J. E. Moore¹, Jason Wachsmann¹, Murthy R. Chamarthy¹, Lloyd Panjikaran², Yuki Tanabe¹, Prabhakar Rajiah¹

¹Department of Radiology, UT Southwestern Medical Center, Dallas, Texas, USA; ²Markey Cancer Center, University of Kentucky, Lexington, Kentucky, USA

Contributions: (I) Conception and design: P Rajiah, AJ Moore; (II) Administrative support: P Rajiah, AJ Moore; (III) Provision of study material or patients: P Rajiah; (IV) Collection and assembly of data: All authors; (V) Data analysis and interpretation: P Rajiah, AJ Moore; (VI) Manuscript writing: All authors; (VII) Final approval of manuscript: All authors.

Correspondence to: Prabhakar Rajiah, MD. Department of Radiology, Cardiothoracic Imaging, UT Southwestern Medical Center, E6.120 B, Mail code 9316, 5323 Harry Hines Boulevard, Dallas, TX 75390-8896, USA. Email: Prabhakar.Rajiah@utsouthwestern.edu.

Abstract: Imaging plays an important role in the evaluation and management of acute pulmonary embolism (PE). Computed tomography (CT) pulmonary angiography (CTPA) is the current standard of care and provides accurate diagnosis with rapid turnaround time. CT also provides information on other potential causes of acute chest pain. With dual-energy CT, lung perfusion abnormalities can also be detected and quantified. Chest radiograph has limited utility, occasionally showing findings of PE or infarction, but is useful in evaluating other potential causes of chest pain. Ventilation-perfusion (VQ) scan demonstrates ventilation-perfusion mismatches in these patients, with several classification schemes, typically ranging from normal to high. Magnetic resonance imaging (MRI) also provides accurate diagnosis, but is available in only specialized centers and requires higher levels of expertise. Catheter pulmonary angiography is no longer used for diagnosis and is used only for interventional management. Echocardiography is used for risk stratification of these patients. In this article, we review the role of imaging in the evaluation of acute PE.

Keywords: Computed tomography (CT); embolism; clot; acute; dual-energy; magnetic resonance imaging (MRI); nuclear; ventilation-perfusion (VQ); angiography; Prospective Investigation of Pulmonary Embolism Diagnosis (PIOPED)

Submitted Oct 19, 2017. Accepted for publication Nov 14, 2017.

doi: 10.21037/cdt.2017.12.01

View this article at: <http://dx.doi.org/10.21037/cdt.2017.12.01>

Introduction

Acute pulmonary embolism (PE) is a common and often fatal complication of venous thromboembolic disease (VTE). Indeed, it is the third leading cause of cardiovascular-related death and responsible for the hospitalization of more than 250,000 patients in the United States annually (1-3). The estimated number of Americans who die from VTE ranges from 60,000 to 100,000, and 10–30% of people die within the first month after diagnosis (4). Imaging plays a pivotal role in the diagnosis and management of these patients. While multi-detector computed tomography (CT) pulmonary angiography (CTPA) is the most commonly used modality in the workup of suspected PE, it is not the only available modality and

may not always be the most appropriate study despite its commonality (5,6). In this article, we review the clinical features of PE, the role of imaging in the diagnosis, the utility of different imaging modalities, and imaging findings in those modalities.

Epidemiology, clinical features, clinical evaluation

Acute PE is a common cause of acute onset chest pain presenting in the emergency room with as many as 1–2 per 1,000 patients potentially affected by VTE (4). The risk of VTE is increased with inherited thrombophilias with 5–8% of US population having one of these high-risk conditions. Recurrence is seen in up to a third of patients with VTE within 10 years, and half may develop

Table 1 Wells score

Malignancy (1.0 point)
Hemoptysis (1.0 point)
History of pulmonary embolism or deep vein thrombosis (1.5 points)
Tachycardia (>100) (1.5 points)
Immobilization (≥3 days) or recent surgery (within 4 weeks) (1.5 points)
Most likely diagnosis is pulmonary embolism; no alternative diagnosis better explains the illness (3.0 points)
Clinical signs and symptoms of deep vein thrombosis (3.0 points)

long term post-thrombotic syndrome (4). The clinical presentation of acute PE is variable. Up to two-thirds of patients may be asymptomatic, or sudden death may be the first presentation. Common clinical presentations of acute PE include chest pain, tachycardia, hypotension, dyspnea, cough, and hemoptysis. Massive PE presents with hypotension, shock, or cardiac arrest. electrocardiography (EKG) changes of S1Q3 pattern, S1Q3T3 pattern, notched S wave in lead V1, inverted T waves, and right bundle branch block may be seen in patients with right heart strain (7). Signs and symptoms of proximal deep vein thrombosis (DVT) include lower extremity swelling, edema, erythema, and pain.

The clinical risk of PE is stratified based on the Wells score (*Table 1*) (8) or the Geneva score. A three-tier model of classification (0–1, low risk; 2–6, moderate risk; >6, high risk) helps risk stratification in a reliable manner (9). A two-tier model (≤4 PE unlikely; >4 PE likely) approach recommends performing a D-dimer test on “PE unlikely” patients and a CT angiography (CTA) for “PE likely” patients (10). D-dimer is a plasmin-derived degradation product which has a high sensitivity and negative predictive value in diagnosis of VTE (11). A negative D-dimer test (<500 ng/mL) in a low or intermediate pre-test likelihood patient excludes acute PE, and no further testing is required. However, if the D-dimer test is positive, then patients should undergo CTA for further evaluation (10). In patients greater than 50 years of age, the D-dimer cut-off has to be adjusted to improve specificity by multiplying the age by 10. Caution should be exercised in patients with sepsis, malignancy, pregnancy, myocardial infarction, or recent surgery as these conditions may result in false positive D-dimer (12).

Imaging techniques in the evaluation of PE

Multiple imaging modalities are available in the evaluation

of acute PE. This includes chest radiographs, CTPA, CT venography (CTV), magnetic resonance (MR) pulmonary angiography (MRPA), nuclear medicine ventilation/perfusion scan, venous ultrasound, echocardiography, and catheter pulmonary angiography. In the following sections, we will discuss each imaging modality, with reference to their advantages, disadvantages, diagnostic role, imaging findings and accuracies.

Chest radiograph

The chest radiograph is not useful in the diagnosis of PE, per se, but it is useful in excluding other causes of acute chest pain such as pneumonia, pulmonary edema, or pneumothorax. However, some relatively specific radiographic abnormalities may be seen in patients with acute PE. An enlarged pulmonary artery, referred to as the Fleischner sign, is secondary to pulmonary hypertension or distension of the vessel by pulmonary embolus. Regional oligemia from PE is dubbed the Westermark sign, and this has 14% sensitivity, 92% specificity, 38% positive predictive value (PPV), 76% negative predictive value (NPV) in diagnosis of PE. In patients with pulmonary infarction, a peripherally located wedge shaped opacity may be seen and is called a Hampton hump (*Figure 1*) (sensitivity 22%, specificity 82%, PPV 28%, NPV 76%). Other non-specific findings include pleural effusion (sensitivity 36%, specificity 70%, PPV 28%, NPV 76%), elevated diaphragm (sensitivity 20%, specificity 85%, PPV 30%, NPV 76%) and vascular redistribution (sensitivity 10%, specificity 87%, PPV 21%, NPV 74%) (13).

VQ scanning

Lung scintigraphy (LS), which refers to the use of radioisotopes for ventilation, perfusion, or both was the

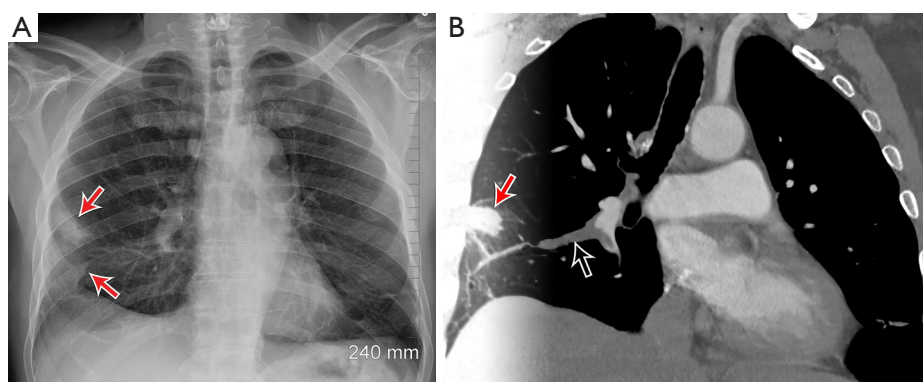


Figure 1 Hampton's hump. (A) Frontal chest radiograph in a 55-year-old male shows a wedge-shaped opacity in the periphery of the right lateral lung (red arrows) concerning for infarction, dubbed a “Hampton hump”; (B) coronal CTPA of the chest shows a filling defect within an enlarged right lower lobe lateral segmental pulmonary artery consistent with occlusive thrombus (black arrow) and a wedge-shaped peripheral opacity consistent with infarct, correlating with abnormality on radiograph (red arrow). CTPA, computed tomography pulmonary angiography.

diagnostic study of choice in PE for about 30 years until newer CT techniques developed (14). Ventilation (V) and perfusion (Q) scans are used in the evaluation of PE, particularly in estimating the likelihood of its presence (15,16). Although CTPA is the current gold standard, there are various clinical situations in which VQ scan is preferred, particularly renal failure, contrast material allergies, young females, and patients who cannot fit into the CT scanner. VQ scan has 50-fold lower radiation dose to the breast (0.28–0.9 *vs.* 50–80 mSv in 64 slice CT) (17,18), which makes it useful in young females, including those who are pregnant. Ventilation agents include aerosolized technetium-99m (Tc-99m) labeled agents [diethylenetriaminepentaacetic acid (DTPA), sulfur colloid, and ultrafine carbon suspensions] and radioactive noble gases [Krypton-81m and Xenon-133 (Xe-133)], with DTPA being the most commonly used agent. Scanning techniques for the various ventilation techniques are variable (15). The results of these agents are comparable, although Tc-99m agents enable multiple views that facilitate regional comparison for ventilation and perfusion. The perfusion portion of the VQ scan is performed following the intravenous injection of 200,000–700,000 particles of Tc-99m labeled macro-aggregated albumin (MAA). Multiple planar images are obtained with the patient in upright position. The use of single-photon emission computed tomography (SPECT)/CT on perfusion imaging can also be considered, which is typically performed using a low-dose CT technique (15). Ventilation scans can be performed before or after the perfusion scan. If perfusion

scan is performed first and it is normal, then the ventilation scan can be avoided, particularly in pregnant patients. With Xe-133 ventilation scans, performing perfusion first provides information on appropriate projections. Perfusion imaging alone is also considered in patients with suspicion of acute PE and sudden clinical deterioration as well as those who cannot remain still or hold his or her breath.

VQ scans are interpreted along with a correlative chest radiograph performed within 12–24 hours. A peripheral wedge-shaped perfusion defect in a lobar, segmental, or sub-segmental distribution without a corresponding ventilation defect (i.e., a mismatched defect) raises the concern for the presence of PE. Mismatched defects can also be seen in other disorders such as congenital vascular abnormalities, vasculitis, veno-occlusive disease, cancer, and mediastinal lymphadenopathy. The etiology of perfusion defects is not always vascular, and they may be secondary to preferential shunting of blood away from a pulmonary parenchymal abnormality. In these cases, the perfusion defect is usually matched by abnormalities on ventilation (i.e., a “matched” defect). It is also commonly matched with a regional chest radiograph abnormality (i.e., a “triple matched” defect). Several schemes are available to categorize the likelihood of PE. The original multicenter Prospective Investigation of Pulmonary Embolism Diagnosis (PIOPED) study classified VQ scans as high-probability, intermediate-probability, low-probability, and indeterminate (19). The gestalt method of interpretation has also been evaluated but is dependent on the reader and their experience (20). Currently, the modified PIOPED II and prospective investigative study of

acute pulmonary embolism diagnosis (PISAPED) criteria are the most commonly used and have fewer non-diagnostic exams compared to prior methods (15,21). The modified PLOPED II criteria classify studies as high probability, very low probability, normal, and non-diagnostic. Normal scans demonstrate homogeneous, diffuse radiotracer activity throughout the lungs on both perfusion and ventilation imaging (Figure 2A). High probability findings include at least two large mismatched segmental defects or segmental defect equivalents (defect >75% of a segment = 1 segment equivalent and 25–75% = 0.5 segment equivalent) (Figure 2B). Very low probability findings include non-segmental defects, 1–3 small segmental defects (small = defect <25% of a segment), a solitary matched defect in the mid or upper lung, the presence of peripheral perfusion in a defect (stripe sign), two or more matched defects with a regionally normal chest radiograph, or a solitary large pleural effusion. All other findings are considered non-diagnostic (15). The sensitivity and specificity of VQ scanning was 85% and 93%, respectively using PLOPED II criteria and 80% and 97% using PISAPED criteria (14,21), which is close to the diagnostic accuracy of CTPA (20). The likelihood ratios of PE being present on a positive VQ scan are 11 for modified PLOPED II criteria, and 23.7 when using PISAPED criteria. When the likelihood ratio was greater than 10, they concluded that the presence of PE was able to be confirmed (22). The sensitivity and specificity can be further improved by using SPECT, which allows for 3D imaging of the pulmonary parenchyma along with extra information that is obtained from CT, however the findings of small peripheral emboli are of unknown significance. The sensitivity and specificity of SPECT were 97% and 91% respectively, compared to CTPA values of 86% and 98% respectively (23). In summary, VQ scan is currently used in select indications, particularly in pregnancy, young patients, contrast material allergy and renal impairment or in outpatients with low probability.

CTPA

CTPA is the imaging modality of choice for the workup of patients with suspected acute PE and is a crucial component in commonly used clinical diagnostic algorithms (5). CTPA has high sensitivity and specificity, with PLOPED II trial demonstrating sensitivity of 83% and specificity of 96%. When combined with clinical probability, the positive predictive value rose to as high as 96% when there was high or low clinical probability and 92% when there was

intermediate clinical probability (24,25). Several other notable advantages of CTPA also engender its widespread adoption. Primarily, it is readily available (26), minimally invasive, and fast with scan duration in modern scanners of less than one second. The incorporation of CTPA has also been found to be a cost-effective solution in the workup of patients with PE when combined with clinical criteria (3). The field-of-view of CTPA is not limited to solely the pulmonary arteries and consequently, beyond simply allowing the direct visualization of thrombus, CTPA can reveal other etiologies of chest pain and shortness of breath such as musculoskeletal injuries, pericardial abnormalities, pneumonia, vascular pathologies, and even coronary artery disease in some protocols (27). Most recognized and of frequent concern of using CT is the theoretical risk of cancer as a result of ionizing radiation; however, advances in protocols and technique as detailed below can render diagnostic studies while minimizing the amount of ionizing radiation. Moreover, Woo *et al.* showed a significant benefit-to-risk ratio of CTPA when taking into account the mean lifetime attributable risk of cancer mortality (28). CTPA is performed with intravenous contrast material, which is associated with contrast-induced-nephropathy (CIN) and may not be suitable for patients with a low glomerular filtration rate (GFR) although the risk is probably overestimated in many clinical scenarios (29,30). Adverse events, including anaphylactoid reactions, related to intravenous iodinated contrast for modern low-osmolar and iso-osmolar contrast materials are low, ranging from 0.2% to 0.7% with fatal reactions occurring in 1 out of 170,000 injections (31–33).

Various CTPA protocols employed to render a diagnostic CTPA study are largely dependent on available hardware but also on reader preference, patient size, patient motion and cardiac function. A diagnostic CTPA should result in adequate opacification of the pulmonary arteries, such that thrombus can be readily distinguished from intraluminal contrast material. A minimum intraluminal density of 93 HU is required for the detection of acute thrombus and 211 HU for chronic thrombus (34). For determining the optimal timing of contrast material bolus, there are three approaches, namely empirical, bolus-tracking and timing bolus. Empirically-derived predetermined amount of time for acquiring images following intravenous administration of contrast material is simple to execute but does not account for varying physiology, scanners and injection rates. In the bolus-tracking method, a region of interest (ROI) is placed over the main pulmonary artery in the axial image and

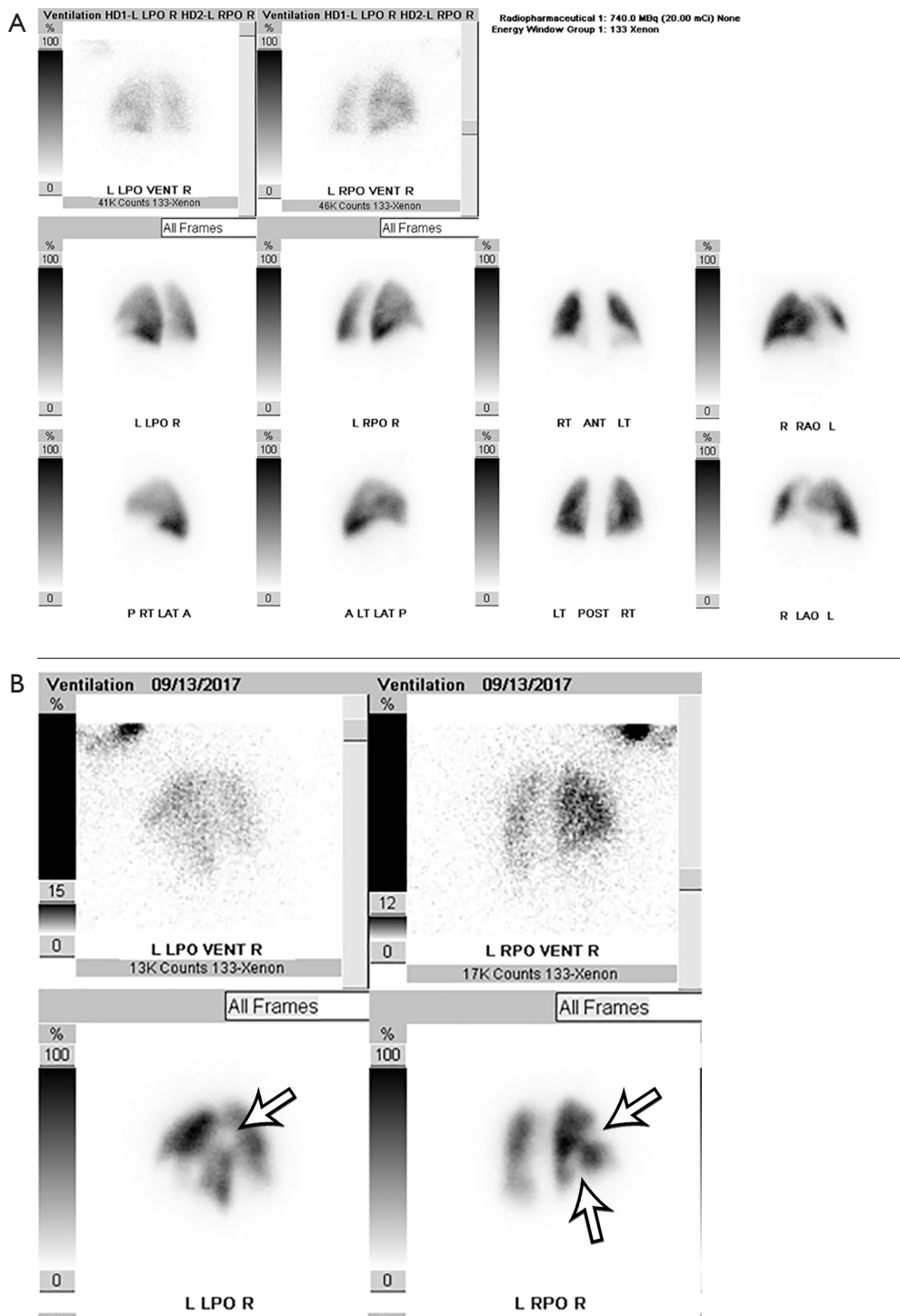


Figure 2 VQ scan findings. (A) Ventilation images obtained following the administration of Xe-133 in LPO and RPO positions and perfusion images in multiple projections obtained following the administration of MAA-Tc-99m show uniform distribution of radiotracer in both phases; (B) ventilation images obtained following the administration of Xe-133 in LPO and RPO positions show no ventilation defect and uniform distribution of radiotracer. Selected LPO and RPO perfusion images following the administration of MAA-Tc-99m show mismatched segmental perfusion defects in the right upper lobe anterior segment, right lower lobe posterior segment, and left upper lobe apico-posterior segment (white arrows). VQ, ventilation-perfusion; LPO, left posterior oblique; RPO, right posterior oblique; MAA, macro-aggregated albumin.

multiple dynamic images are obtained in the same position after injection of contrast material. When a pre-determined threshold is met (e.g., 100 HU), scanning is initiated, typically with a preset delay to allow maximum opacification. This method requires little input from the technologist and can ensure reproducibility across multiple centers. In the timing bolus technique, a small bolus of contrast material (10 mL) is injected at the desired rate, followed by a dynamic scan with a ROI over the pulmonary artery. A time-attenuation curve is generated, the time-to-peak opacification is determined and the scan delay time is calculated by adding a few seconds to account for the larger amount of contrast material that will be utilized in the diagnostic portion of the study and the time taken for scanner to move to the start position. Typically, 60 to 150 mL of intravenous contrast is administered at a rate near 5 mL/s, followed by a saline chaser at the same rate to allow washout of contrast from the superior vena cava (SVC), thus minimizing streak artifact. The exact contrast material volume and rate will vary from scanner to scanner; a greater number of detectors will typically require a smaller amount of contrast material and a higher rate of injection (35). The entire chest is covered in the scan including the subcutaneous tissue, except for pregnant patients where the lung bases can be excluded to minimize radiation dose. Caudo-cranial direction of scanning ensures adequate contrast material in the lower pulmonary vessels and to minimize streak artifact from contrast material in the superior vena cava or brachiocephalic vein (35). Patient should be able to tolerate a short breathhold in inspiration and follow breathing directions adequately to minimize motion artifact. In addition to communication barriers, prolonged deep inspiration results in suboptimal pulmonary artery opacification (36), due to a larger influx of non-opacified blood through the inferior vena cava (IVC) (37), exacerbated by inadvertent Valsalva maneuver, which impedes the inflow of contrast material or a saline chaser into the superior vena cava due to high intrathoracic pressure. End-expiratory technique may render a study diagnostic when inspiratory scans have been suboptimal, although lung parenchymal imaging is inferior (36,38). EKG gating minimizes cardiac motion artifact in the lingula and right middle lobe but has been shown to have little effect on diagnostic accuracy for CTPA evaluation (39). It can be beneficial, however, in instances when other pathology such as coronary artery disease or aortic root pathology are also being considered (27).

Direct findings of acute PE in CT include a central

filling defect within a vessel surrounded by contrast material yielding a “polo mint” appearance when orthogonal to the long axis of the vessel or a “railway sign” when observed parallel to the vessel long axis (*Figure 3A,B*). An eccentric or mural filling defect rendering an acute angle with a vessel wall or complete occlusion of a dilated vessel by a filling defect can also be seen (*Figure 3C*). When particularly large and draped over the pulmonary trunk bifurcation, the embolus may be referred to as a “saddle embolus” (*Figure 3D*) (40,41). CTPA can detect very small sub-segmental pulmonary emboli which can be sub millimeter (*Figure 3E*). Pulmonary infarct is a notable consequence of acute PE and manifests on CTPA as wedge-shaped, peripheral opacity commonly with a “reverse-halo” or “atoll” appearance consisting of central ground glass and a rim of consolidation (*Figure 4A*). Pleural effusions can also be seen with acute PE (42). These findings are distinct from chronic PE, which manifests as intraluminal webs, calcification, thrombus recanalization, and filling defects adherent to the wall that form obtuse angles and concave surfaces. In chronic PE, the vessels are typically smaller than normal, exhibit abnormal tapering, and may show complete cut-off of the segmental vessel. Parenchymal changes of chronic PE include mosaic perfusion, band-like opacities, and bronchial dilation in abnormal areas (40,43).

CT provides several parameters for estimating the severity of PE and risk-stratification, such as right heart strain, clot burden and lung perfusion. Features of right heart strain include-increased right ventricle (RV)/left ventricular (LV) ratio (>1 in axial plane, >0.9 in 4-chamber reconstruction), flattening of interventricular septum and reflux of contrast material into the IVC and hepatic veins. RV/LV ratio >1.1 has been associated with increased risk of death within 30 days (44). Four-chamber RV/LV ratio >0.9 (*Figure 4B*), combined with high-sensitivity-cardiac-troponin-I was associated with poor clinical outcome in one retrospective study (45). Another study showed that 3D RV/LV volume ratio >1.2 was predictive of 30-day outcome (46). There are several scores used for quantification of the clot, such as the CT severity score and CT obstruction index developed by Mastora and Qanadli *et al.* respectively, but these are not routinely used in clinical practice (47,48). Perfusion scores are discussed in section on dual-energy CT below.

Technical advances

Several advances in CT technology enable CTPA acquisitions with low radiation and contrast material doses

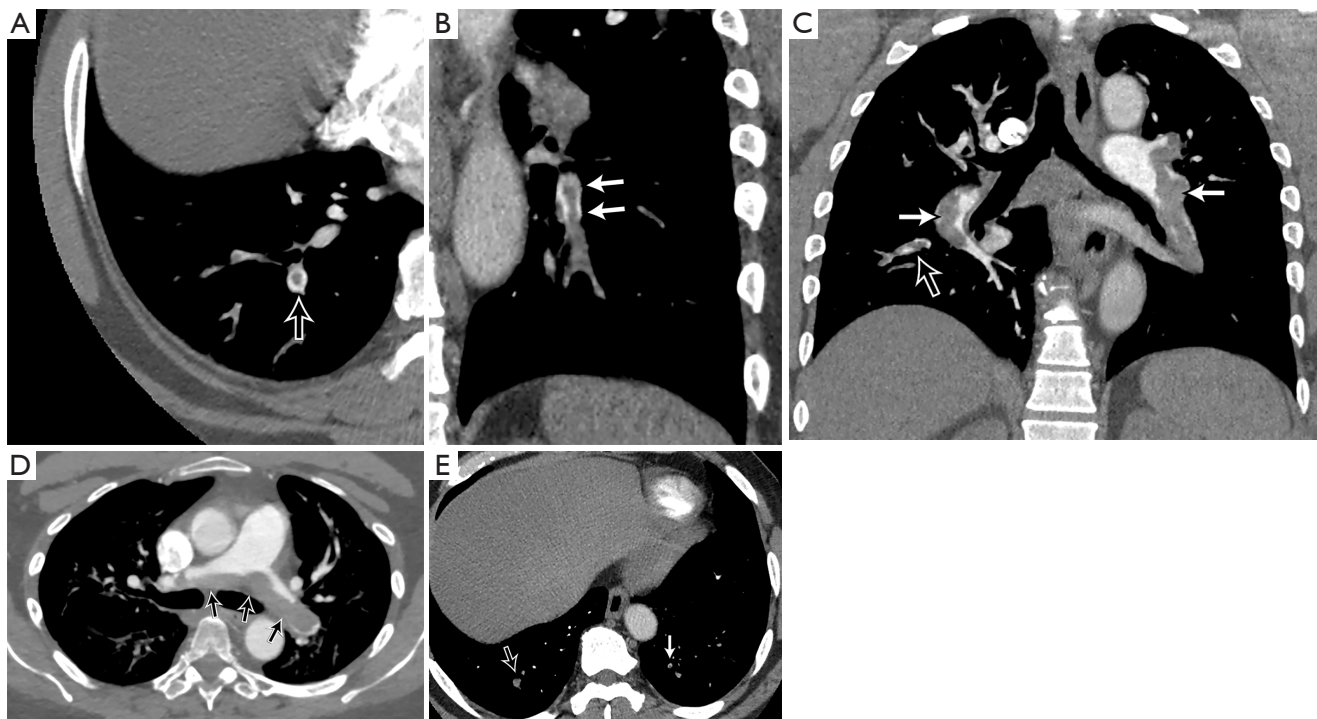


Figure 3 Direct findings of acute PE on CTPA. (A) Axial CTPA orthogonal to an expanded right lower lobe posterior segmental pulmonary artery shows a central filling defect surrounded by a ring of contrast exhibiting the “polo mint” sign of acute PE (black arrow); (B) coronal CTPA oriented along the long axis of a right lower lobe segmental pulmonary artery shows a central filling defect surrounded by parallel lines of contrast consistent with the “railway sign” of acute PE (white arrows); (C) coronal CTPA shows extensive burden of large pulmonary emboli manifested by occlusive and mural filling defects whose edges form acute angles with the vessel walls (white arrows); (D) a large conglomeration of low density embolus is draped over the bifurcation of the pulmonary artery, exhibiting a “saddle embolus” configuration (black arrows); (E) axial CTPA of the lung bases show a dilated right lower lobe posterior basal sub-segmental pulmonary artery with an occlusive filling defect consistent with acute PE (black arrow). There is also a PE in small left lower lobe posterior basal sub-segmental pulmonary artery (white arrow). CTPA, computed tomography pulmonary angiography; PE, pulmonary embolism.

(volume/concentration). Radiation doses can be minimized by using the least possible tube voltage and tube current, based on the body mass index of the patient. Automated parameter selection is now possible with some vendors. Decreasing peak kilovoltage from 120 to 100 kVp in a chest CT results in >30% reduction in radiation dose (49). Tube current can be modulated according to the thickness and density of the part imaged, with estimated radiation dose savings of 26% (50). Such low tube current and voltage studies were traditionally limited by the image noise; however, this is currently mitigated by using advanced iterative reconstruction (IR) algorithms, which uses statistical, model or hybrid techniques (51). Reduced-dose CTPA, when combined with this reconstruction method, has been found to be of similar quality to conventional standard dose CTPA (52). Low contrast material dose

(volume/concentration) can be used in techniques that use lower tube voltage, since at these energies, the effective energy of the X-ray spectra approaches the K-edge of iodine (33 keV), which improves the attenuation of iodine due to photoelectric effect (53). Low voltage scans have been shown to reduce contrast material requirement by 33% with maintained image quality and diagnostic accuracy (54,55). Low radiation and contrast material dose studies are limited in large patients.

With latest generation of dual source scanners which have two X-ray tubes, it is possible to perform high-pitch CT acquisitions (up to 3.4) without gaps in data. The rapid acquisition results in lower radiation dose as well as contrast material volume, since contrast material is needed only for a brief period of time (56,57). Such fast scanning times help to reduce motion artifact and it is now possible to obtain

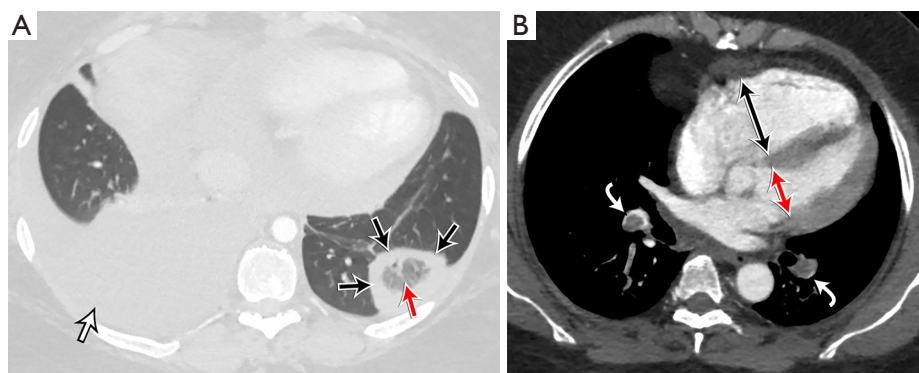


Figure 4 Sequelae of acute PE on CTPA. (A) Axial CTPA demonstrates a round opacity in the left lower lobe posterior segment that exhibits a ground glass center (red arrow) surrounded by a rim of consolidation (black arrows). This is the so-called “reverse halo sign” consistent with pulmonary infarction. There is also a large right pleural effusion (white arrow), a common finding in acute PE; (B) four-chamber CTPA reformation demonstrates a RV/LV ratio (RV, black; LV, red arrow) of greater than 1, indicative of right heart strain. There is extensive embolic burden in the dilated segmental and lobar pulmonary arteries (curved white arrows). PE, pulmonary embolism; CTPA, computed tomography pulmonary angiography; RV, right ventricle; LV, left ventricular.

free-breathing CTPA studies (58). This technique also allows non-gated “triple rule out” studies that evaluate the pulmonary vessels, aorta, and coronary arteries (59). The latest CT protocols combine the improved iodine detection and high-pitch of dual-source dual energy computed tomography (DECT) to render diagnostic CTPA with contrast material loads as low as 20 mL, a tube voltage of 80 to 100 kVp, and tube-current reduction to as low as 80 mAs rendering an effective dose below 1 mSv without significant degradation in image quality (60,61). One prospective, randomized trial of 100 non-obese patients combined low dose technique (80 kVp, 100 mAs) with high-pitch technique to allow free-breathing scans and showed these were non-inferior to standard pitch and dose scans (62). With technological advances involving X-ray tube power and IR algorithms, it may be even possible to do high-pitch CTPA even in large patients without noise limitations (63). Patient specific contrast material formula and exponentially decelerated contrast material injection rate is another technique of reducing contrast load, but this involves complex calculations and not feasible for routine clinical implementation (64).

DECT

DECT uses two energy levels to create data sets from two distinct X-ray spectra, which can be used to distinguish materials based on their unique interactions with the differing X-ray energy spectra. Higher molecular weight

materials show a greater difference in X-ray attenuation when exposed to low and high energy levels as compared to lower molecular weight materials, due to the higher probability of the photoelectric effect in high molecular weight materials when interacting with lower energy X-rays (65,66). Several technologies of dual-energy CT are available, some operating at the source level (dual-source, rapid kVp switching, dual-spin, split-beam) and others at the detector level (dual-layer, photon counting CT) (66-68). Data sets derived from DECT can be used to generate iodine maps that, in turn, allow visualization of the distribution of iodine within the lung after intravenous contrast material administration. Using post-processing software, perfusion maps can be generated to overlay traditional CT images following which, quantitative volume analysis or ROI analysis can be performed. Some vendors are able to generate pulmonary perfused blood volume (PBV) images (*Figure 5*). Typically, concentration of iodine greater than 300 mg I/mL and a slightly longer acquisition, up to 7 seconds, is necessary (69). Wedge-shaped perfusion defects are seen in acute PE, which has been shown to correlate well with pulmonary perfusion on scintigraphy (70). Addition of the perfusion CT to CTPA has been shown to improve the detection of peripheral clots (71). Perfusion defects also correlate with other signs of right ventricular dysfunction (including RV/LV diameter, CT obstruction score) and pulmonary artery obstruction (70,72,73). Semi-automated volumetric quantification of perfusion defects can aid in the prediction of adverse clinical outcomes (74), and fully automated quantitative analysis has

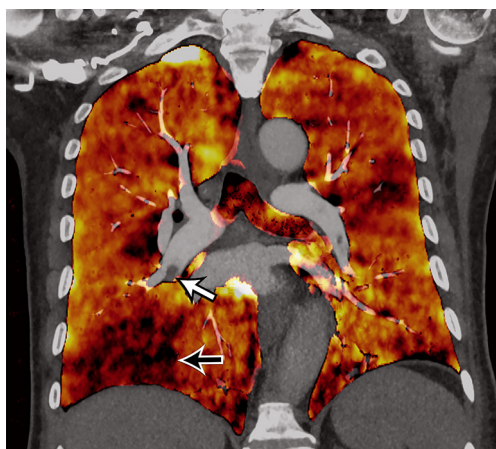


Figure 5 DECT pulmonary perfused blood volume imaging. Coronal CTPA fused with a generated PBV iodine map shows a wedge-shaped perfusion defect in the right lower lobe (black arrow) caused by an acute pulmonary embolus in the distal right interlobar pulmonary artery (white arrow). DECT, dual energy computed tomography; CTPA, computed tomography pulmonary angiography.

shown efficient estimation of PBV which inversely correlates with thrombus amount, clinical findings of severe PE, and ICU admission (75).

Dual-energy CT also allows the use of virtual monoenergetic images (VMI). VMI at low energy levels (40–70 keV) have higher image contrast, which can be used to salvage suboptimal study or prospectively use low iodine dose (volume/concentration) with up to 50% reduction in iodine concentration (76–78). Optimal energy level may vary depending on the scan technology. VMI at high energy levels can be used to minimize artifacts. Virtual non-contrast image (VNC) can also be obtained from DECT, which can be used as a problem-solving tool for characterizing incidental lesions. For example, a high attenuating lesion in the mediastinum could be either contrast material or an inherently high-density material such as a surgical material. This can be distinguished based on VNC.

Lower extremity ultrasound

Lower extremity ultrasound (US) is an important step in the diagnostic algorithm for suspected VTE (79) and has replaced contrast-enhanced venography as the standard of practice in the evaluation of patients suspected to have DVT. The widespread availability, lack of ionizing radiation, and low cost are highly advantageous components of US. It

can also identify non-vascular etiologies of pain such as calf edema, Baker's cysts, hematoma, and infection. The most proximal and pelvic veins cannot be imaged adequately by US, and patient limiting factors such as surgical wounds, casts, and body habitus may preclude thorough examination of the venous structures. Typically, the veins of interest are imaged in greyscale B mode which can identify the direct features of intravascular thrombus. This is most often combined with dynamic compression ultrasound whereby the vein in question is viewed in cross-section and compressed by the sonographer in real-time. This technique can be employed alone, referred to as limited compression US, or in combination with color Doppler and spectral Doppler. Color and spectral Doppler used alone are referred to as duplex US while the combination of color, spectral, and compression US is referred to as triplex US (80). Some centers include as part of their protocol the observation of flow augmentation (or lack thereof) on spectral Doppler during manual compression of the calf (79).

There is debate in the literature about the appropriate anatomic coverage necessary for the exclusion of clinically relevant lower extremity DVT on US (81). Primarily, US of the whole lower extremity can be employed or US limited to the lower extremity proximal to the calf. It is becoming common clinical practice for clinicians performing bedside ultrasound to employ a two-point strategy whereby only the common femoral and popliteal veins are evaluated with compression US alone. When this is negative but there is a positive D-dimer, a 1-week follow-up whole-leg US is performed (82). One multicenter study of 2,098 patients comparing this serial two-point strategy and whole-leg US suggested that these approaches are clinically equivalent with similar rates of VTE at 3 months follow-up (0.9% for serial two-point US and 1.2% for whole-leg US) (83).

Acute deep vein thrombus manifests on US as hypoechoic intravascular material that expands the venous lumen. DVT may be fully occlusive or non-occlusive, and the affected vessel lumen will not collapse under compression (*Figure 6*) (84). Color Doppler may be useful to demonstrate a lack of flow, but caution with this approach is recommended as blooming of color maps may obscure small thrombus. Spectral Doppler waveforms can be observed for appropriate response to calf compression; a lack of response being indicative of intervening thrombus between the point of observation and the calf. Lack of normal respiratory phasicity of the more proximal veins may indicate central venous thrombus. The sensitivity and specificity of US is highly dependent on technique and operators. A 2005



Figure 6 Lower extremity ultrasound findings of acute DVT. Long axis views of the left common femoral vein and great saphenous vein confluence. B mode grayscale imaging (left) shows a mixed echogenicity material filling the entirety of both veins (red arrows) consistent with acute thrombus. Color Doppler imaging (right) showed no discernable flow. Dynamic compression (not shown) showed no change in caliber of the venous structures. Findings are consistent with acute DVT. DVT, deep vein thrombosis.

meta-analysis of 100 cohort studies showed that duplex and triplex US offers a sensitivity of 96% each for proximal DVT, 71% and 75% respectively for distal DVT, and an overall specificity of 94% each. Compression US alone was more specific but less sensitive and demonstrated proximal sensitivity of 96%, distal sensitivity of 75%, and overall specificity of 98% (80).

CTV

CTV can also be used in the detection of deep vein thrombosis in the extremities. It can be obtained at the same time of CTPA, limiting the need for additional time-consuming studies, and unlike US, CTV can be performed adequately in patients with overlying casts, surgical material, or wounds. It also allows imaging of the more central venous structures which can be challenging with lower extremity US, and additional sources of leg pain can be identified beyond the realm of the vascular structures (85). In the PIOPED II trial, combined CTPA and CTV increased sensitivity for thromboembolic disease to 90% from 83% (although it decreased specificity to 95% from 96%). Moreover, it was also recommended in combination with CTPA as part of that study's conclusion. The radiation dose of CTPV ranges from 4.8 and 9.7 mSv, effectively doubling the total radiation dose compared to CTPA alone (86). In order to reduce radiation exposure, imaging of the central venous structures (the iliac veins and inferior vena cava) was not recommended which arguably diminishes the advantage of CTV over US (87). CTV also requires the use of a greater volume of intravenous contrast material, the

disadvantages of which were discussed previously.

CTV, when performed as part of a diagnostic algorithm for PE, is obtained following CTPA and is sometimes referred to in the literature as "indirect CTV." In the PIOPED II trial, a helical acquisition using 7.5 mm reconstructions, a pitch of 1.5, and tube current of 180 mA and 120 kVP (or 140 kVP in larger patients) was utilized. Images were obtained from the iliac crest through the level of the tibial plateau at a delay of 3 to 3.5 minutes (88). An alternative approach is to use axial technique to lower radiation with noncontiguous 5 mm slices at 4 cm intervals. The patient's feet may be elevated to ensure speedy return of venous contrast material by avoiding compression of the calf veins (84,89). The exam can also be limited to just the pelvis if the goal is to evaluate the most central venous structures where ultrasound is less effective (86). Superior venous enhancement can be obtained with a lower tube voltage of 100 kVP; a lower voltage of 80 kVP was found to be impractical due to lengthy scanner times and scanner hardware limitations (53). A recent prospective study of 96 patients used an approach that combined indirect CTV with direct CTV by adding a second injection of contrast material directly into the dorsal vein of the diseased limb. Using dual-source CT and fast-pitch technique, this yielded sensitivity of 95–97% and a specificity of 100% when compared to combination US and digital subtraction angiography (90).

Acute DVT on CTV appears as a complete or partial filling intraluminal hypodense filling defect in a deep vein. The vein is typically expanded, and a rim of enhancing venous wall may be seen. Secondary signs include edema

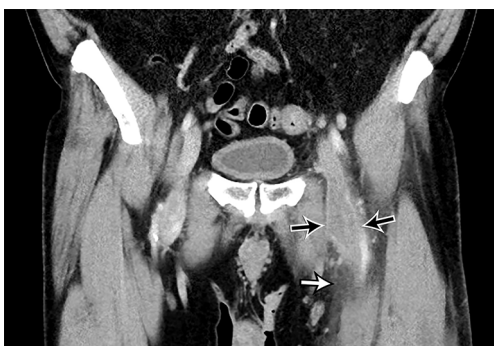


Figure 7 CTV findings of acute DVT. Coronal CTV image shows a central filling defect within the expanded left common femoral artery (black arrows). The presence of stranding in the surrounding fat is an additional clue as to the diagnosis (white arrow). DVT, deep vein thrombosis.

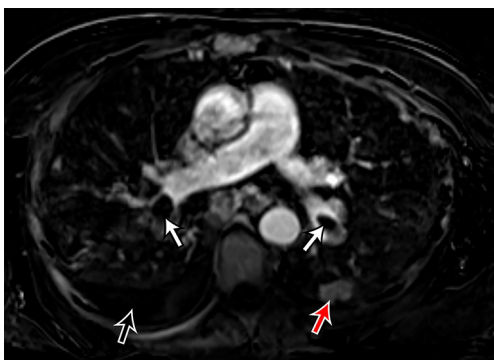


Figure 8 MRI findings of acute PE. Axial T1-weighted fat saturated MR angiographic sequence with digital subtraction show low signal filling defects within the right pulmonary artery and left common basal pulmonary artery consistent with acute PE (white arrows). There is also a small right pleural effusion (black arrow) which is often seen with acute PE and a metastasis from colorectal cancer in the posterior left lung (red arrow). MRI, magnetic resonance imaging; PE, pulmonary embolism.

in the adjacent tissues (*Figure 7*). Chronic DVT manifests on CTV with small vessels, recanalization of thrombus, calcifications, and thickened venous veins (84,88). The mean CT attenuation of DVT is between 31 and 65 HU (53). The use of CTV as an adjunct to CTPA has had variable reception in the literature. CTV in some literature has also shown to have both poor sensitivity and specificity compared with ultrasound (89), and an early study even recommended confirmation of CTV findings with US due to the CTV's poor positive predictive value (91). At the

least, US has been shown to be of equivalent diagnostic value bringing into question the practical routine usage of CTV (88). While the PIOPED II trial recommended CTV in combination with CTPA, recent literature argues against its routine use owing to its negligible advantage over CTPA alone and the disadvantage of extra ionizing radiation and cost. It may be of benefit, though, in patients for whom their comorbidities place them at increased mortality risk if a lower extremity thrombus is missed (86,92).

MR angiography (MRA)

The significant development of magnetic resonance imaging (MRI) technology has enabled faster sequences, with high contrast and spatial resolution. MRI can provide both morphological and functional information. MRI protocols consist of: free-breathing steady-state free precession sequence for PE; post-contrast T1-weighted 3D-contrast enhanced MRA for pulmonary angiogram; T1-weighted 4D-contrast enhanced first pass perfusion study for lung perfusion; and T1-weighted volumetric interpolated 3D gradient-echo for mediastinal and pleural disease (93,94). MRPA findings of PE include filling defects, complete absence of vessel enhancement, dilatation of the main pulmonary artery, and caliber change with post-stenotic dilatation (*Figure 8*) (95,96). In comparison with CTPA, MRPA had lower sensitivities for detecting PE, especially in peripheral pulmonary arteries (97,98). According to the results of PIOPED III study, MRPA had a sensitivity of 78% and a specificity of 99% for detecting VTE (with exclusion of the technically inadequate group), but the sensitivity decreased in the detection of smaller emboli (sensitivity 79% in the main or lobar pulmonary arteries *vs.* 50% in the segmental arteries and 0% in the sub-segmental arteries) (99). The major limitation of MRPA in this trial was the large proportion of technically inadequate results and the investigators indicate that MRPA should be considered only in well-experienced facilities and only for patients with contraindications to standard tests (99). MRPA might be appropriate instead of CTPA and VQ scintigraphy only in patients with intermediate pretest probability with a positive D-dimer or high pretest probability (100). Indeed, MRPA is not used in clinical routine as CTPA because of the technically inadequate studies, less robustness, long examination times, and contraindication to MRI in patients with implanted devices and claustrophobia, and limited ability of MRPA to detect cardiopulmonary disorders other than PE.

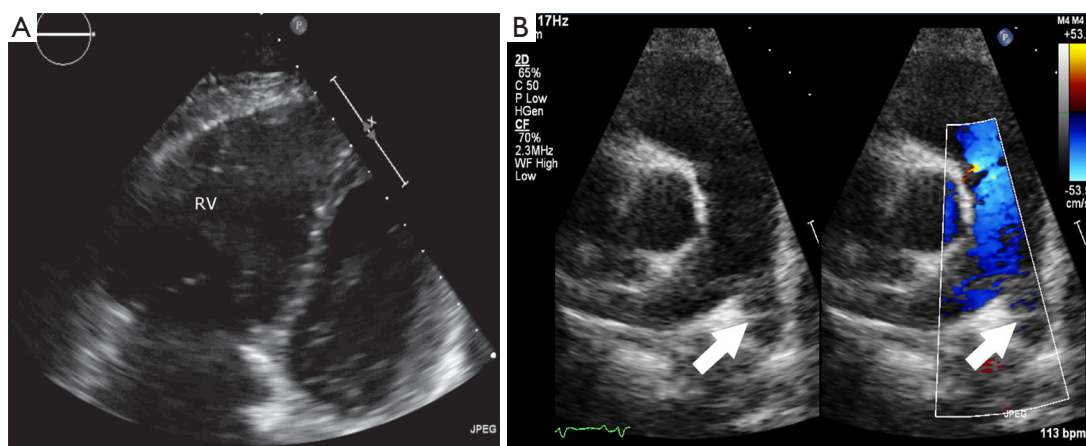


Figure 9 Echocardiographic findings of acute PE. (A) Trans-thoracic echocardiogram in a patient with acute sub-massive PE demonstrates dilated RV; (B) trans-thoracic echocardiogram in another patient demonstrates thrombus within the left pulmonary artery at the bifurcation of pulmonary trunk (arrow). PE, pulmonary embolism; RV, right ventricle.

MRI allows for visualization of PE on pulmonary perfusion images as areas of reduced, delayed, or absent blood flow. MR perfusion imaging has a high sensitivity for detecting PE and it is often used in combination with MRPA (94). Hemodynamic parameters, such as forward flow, retrograde flow, average velocity and peak velocity, can be also obtained using velocity-encoded phase contrast sequences (101). Moreover, MRI allows for an accurate and reproducible assessment of the right and left ventricular myocardial function, hypertrophy, and fibrosis described as delayed enhancement (102,103). Nevertheless, the further development of MRI technology and more evidence are needed for the clinical use of MRI to evaluate acute PE.

Echocardiography

Transthoracic echocardiography (TTE) has limited sensitivity and specificity for diagnosis of acute PE. A negative echocardiogram cannot exclude a diagnosis of PE, and similarly positive findings can be secondary to cardiorespiratory disease in the absence of PE. However, there is significant role for exclusion of other confounding diagnoses, identification of high risk patients for emergent thrombolysis, prognostic prediction and monitoring response to therapy (104). Presence of RV dysfunction, right-to-left shunt, and right ventricular thrombus are each associated with approximately two-fold increased risk of mortality whereas normal echocardiogram is associated with excellent outcomes (105). TTE findings in PE are usually indirect and a comprehensive evaluation is required (106).

Presence of right sided cardiac thrombus, dilated diastolic RV diameter >30 mm or $RV/LV >1$, systolic flattening of interventricular septum or acceleration time <90 ms or TI gradient >30 mmHg in absence of RVH represent the RV overload criteria and are seen in 30–40% of patients with PE (107) (Figure 9). The 60/60 sign (RVOT AT ≤ 60 ms in presence of TI gradient ≤ 60 mmHg), and McConnell sign (RV free wall hypokinesia/akinesia with preserved apical segment wall motion) are highly specific with high PPV even in presence of previous cardiorespiratory disease (108,109).

Echocardiographic evaluation is currently not recommended for a hemodynamically stable patient with suspected PE. However, in patients suspected with high-risk PE, echocardiography can differentiate and triage multiple etiologies resulting in hemodynamic instability. Absence of RV overload or dysfunction can exclude PE as cause of the hemodynamic instability. More importantly, it can establish the need for emergent treatment by demonstrating RV overload and dysfunction, or right heart thrombi. Transesophageal echocardiography (TEE) is highly specific and can directly visualize pulmonary thromboembolism rendering a prompt diagnosis, although absence of thrombus does not exclude PE. Pruszczyk *et al.* reported a sensitivity of 80.5% and a specificity of 97.2% for TEE in detection of thromboembolic disease for suspected PE patients with signs of RV overload on TTE (110). TEE performs better compared to TTE, however is limited by operator dependence and technical factors. TEE remains the diagnostic study of choice for a quick bedside evaluation



Figure 10 Angiographic findings of acute PE. (A) Pulmonary arteriogram in a 34-year-old female with hemodynamically unstable PE demonstrates multiple filling defects throughout the pulmonary arteries including complete cutoff of the right interlobar artery (arrow), and occlusion of right upper lobar artery, left lower lobe pulmonary artery, and lingular branch; (B) large right upper lobe filling defect in a different patient consistent with acute PE (arrow). Also noted are areas of decreased perfusion within the peripheral upper and lower lobes consistent with sub segmental emboli. PE, pulmonary embolism.

of PE in high risk patients with RV dysfunction (on TTE) or hemodynamic instability [shock/hypotension, pulseless electrical activity (PEA), cardiac arrest] (111).

Conventional pulmonary angiography (CPA)

CPA was the reference standard for the diagnosis of PE in PIOPED I and PIOPED II trials (25,112). However, it is an invasive procedure and has limited role for PE diagnosis in the modern era of multi-detector CT. It is now used only when a concomitant endovascular treatment is planned. An isolated CPA is rarely performed, when the imaging diagnosis is inconclusive or clinically discordant. CPA findings of PE include occlusion with abrupt cut-off, filling defects, slow flow, and regional hypo-perfusion (*Figure 10*). Angiographic severity indices were proposed to quantify the severity of PE (113,114). Peripheral, small, sub-segmental filling defects may also be identified; however, there is high inter-observer variability, and accuracy may be inferior to CTPA at these levels (112,115,116).

A right common femoral or internal jugular vein approach is utilized to access the pulmonary artery with a 7 Fr sheath placed within the accessed vein. Catheter-directed endovascular interventions at times require two accesses or a larger sheath. An angled/regular pigtail catheter can be utilized to navigate through the right atrium (RA), RV and pulmonary artery. Transient arrhythmias are common

while navigating within the right heart, and care should be exercised to quickly advance or pull back wires and catheters. Likewise, temporary pacing is indicated if a pre-procedure EKG demonstrates a left bundle branch block. Pulmonary arterial and right atrial pressure measurements are obtained prior to angiography and are helpful for risk stratification and prognosis. Selective right and left pulmonary arteriograms are performed with multiple oblique views (and magnification views as needed) using injection rate of 25 mL/s and contrast material volume of 40–50 mL; however, the rate and volume of injection are decreased in patients with pulmonary hypertension. Alternatively, a hand injection can be considered in acute PE. CPA is associated with 2% mortality and a 5% morbidity (117). Complications are related to access site (bleeding, hematoma), catheter/wire injury (arrhythmias, cardiac perforation), contrast nephropathy, and thrombolysis [bleeding, disseminated intravascular coagulation (DIC)] (118).

Diagnostic algorithm for acute PE

Combining imaging with a clinical pretest assessment of the probability of PE yields superior sensitivity and specificity than imaging alone as shown in PIOPED II trial (87). Pre-test probability is based on the Wells deep vein thrombosis score, Wells PE score, or revised Geneva score, after which

laboratory testing or imaging is pursued. In patients in whom DVT or PE is unlikely, D-dimer testing is pursued. If this is normal, then DVT or PE are excluded. If it is positive, either US or CTPA is recommended. In patients in whom DVT or PE is considered likely based on clinical score, imaging is recommended without the intermediate D-dimer testing step (119).

According to the American College of Radiology (ACR) appropriateness criteria, in patients with a low/intermediate pretest probability and a negative D-dimer test, PE can be safely excluded without further imaging. Nevertheless, a CTA chest is given a rating of 5 indicating it “may be appropriate.” Radiograph is given a rating of 9, or “usually appropriate,” to exclude other causes of chest pain, while other imaging methods are deemed inappropriate. For patients with a positive D-dimer test or high pretest probability, a CTA chest and chest radiograph are given the highest appropriateness rating of 9. A VQ scan is also deemed “usually appropriate” with a score of 7 and should be considered as an alternative to CTA. Ultrasound is given the same rating and may be the initial study prior to CTA. MRA chest without and with contrast or a combined CTPA and CTV may be appropriate with scores of 6 and 5 respectively. For pregnant patients with suspicion of PE, tests with ionizing radiation are generally avoided. US receives a rating of 8, “usually appropriate” and is recommended as the initial imaging modality, particularly when signs and symptoms of lower extremity DVT are present. CTPA or alternatively a VQ scan is still considered usually appropriate and both receive a rating of 7. The ventilation portion of the exam should only be performed if absolutely needed. Although the fetal exposure from both CTPA and VQ scan is low (<1 mGy), there is less fetal radiation exposure with CTPA, particularly in the first trimester (120). However, CTPA delivers greater effective dose to the breast tissue than VQ scan (10–70 mGy for CT *vs.* <1.5 mGy for VQ) (120). MRA is deemed usually not appropriate with a score of 3. Moreover, there is potential risk to the fetus due to gadolinium exposure (100).

Conclusions

CTPA is the current gold standard in the diagnosis of acute PE with high accuracy, wide availability, and rapid turnaround time. Combining CTPA with clinical pre-test probability of PE yields superior sensitivity and specificity than imagining alone. VQ scanning is indicated in patients who are young, pregnant or cannot get contrast. Chest

radiographs are useful in excluding other causes of chest pain. MRPA can provide good accuracy in centers with adequate expertise. In pregnant patients, lower extremity ultrasound is recommended as the initial imaging modality. Echocardiography is useful in triaging high-risk PE patients. Invasive pulmonary angiography is reserved for those patients needing endovascular intervention.

Acknowledgements

None.

Footnote

Conflicts of Interest: The authors have no conflicts of interest to declare.

References

1. Jaff MR, McMurtry MS, Archer SL, et al. Management of massive and submassive pulmonary embolism, iliofemoral deep vein thrombosis, and chronic thromboembolic pulmonary hypertension: a scientific statement from the American Heart Association. *Circulation* 2011;123:1788-830.
2. Ruggiero A, Sreaton NJ. Imaging of acute and chronic thromboembolic disease: state of the art. *Clin Radiol* 2017;72:375-88.
3. Raymakers AJ, Mayo J, Marra CA, et al. Diagnostic strategies incorporating computed tomography angiography for pulmonary embolism: a systematic review of cost-effectiveness analyses. *J Thorac Imaging* 2014;29:209-16.
4. Beckman MG, Hooper WC, Critchley SE, et al. Venous thromboembolism: a public health concern. *Am J Prev Med* 2010;38:S495-501.
5. Goldhaber SZ, Bounameaux H. Pulmonary embolism and deep vein thrombosis. *Lancet* 2012;379:1835-46.
6. Wiener RS, Schwartz LM, Woloshin S. When a test is too good: how CT pulmonary angiograms find pulmonary emboli that do not need to be found. *BMJ* 2013;347:f3368.
7. Zhan ZQ, Wang CQ, Nikus KC, et al. Electrocardiogram patterns during hemodynamic instability in patients with acute pulmonary embolism. *Ann Noninvasive Electrocardiol* 2014;19:543-51.
8. Wells PS, Anderson DR, Rodger M, et al. Excluding pulmonary embolism at the bedside without diagnostic imaging: management of patients with suspected pulmonary embolism presenting to the emergency

- department by using a simple clinical model and d-dimer. *Ann Intern Med* 2001;135:98-107.
9. Wolf SJ, McCubbin TR, Feldhaus KM, et al. Prospective validation of Wells Criteria in the evaluation of patients with suspected pulmonary embolism. *Ann Emerg Med* 2004;44:503-10.
 10. van Belle A, Buller HR, Huisman MV, et al. Effectiveness of managing suspected pulmonary embolism using an algorithm combining clinical probability, D-dimer testing, and computed tomography. *JAMA* 2006;295:172-9.
 11. Schrecengost JE, LeGallo RD, Boyd JC, et al. Comparison of diagnostic accuracies in outpatients and hospitalized patients of D-dimer testing for the evaluation of suspected pulmonary embolism. *Clin Chem* 2003;49:1483-90.
 12. Righini M, Van Es J, Den Exter PL, et al. Age-adjusted d-dimer cutoff levels to rule out pulmonary embolism: The adjust-pe study. *JAMA* 2014;311:1117-24.
 13. Worsley DE, Alavi A, Aronchick JM, et al. Chest radiographic findings in patients with acute pulmonary embolism: observations from the PIOPED Study. *Radiology* 1993;189:133-6.
 14. Anderson DR, Barnes DC. Computerized tomographic pulmonary angiography versus ventilation perfusion lung scanning for the diagnosis of pulmonary embolism. *Curr Opin Pulm Med* 2009;15:425-9.
 15. Parker JA, Coleman RE, Grady E, et al. SNM practice guideline for lung scintigraphy 4.0. *J Nucl Med Technol* 2012;40:57-65.
 16. Sinzinger H, Rodrigues M, Kummer F. Ventilation/perfusion lung scintigraphy. Multiple applications besides pulmonary embolism. *Hell J Nucl Med* 2013;16:50-5.
 17. Mattsson S, Johansson L, Leide Svegborn S, et al. Radiation dose to patients from radiopharmaceuticals: a compendium of current information related to frequently used substances. *Ann ICRP* 2015;44:7-321.
 18. Einstein AJ, Henzlova MJ, Rajagopalan S. Estimating risk of cancer associated with radiation exposure from 64-slice computed tomography coronary angiography. *JAMA* 2007;298:317-23.
 19. Webber MM, Gomes AS, Roe D, et al. Comparison of Biello, McNeil, and PIOPED criteria for the diagnosis of pulmonary emboli on lung scans. *AJR Am J Roentgenol* 1990;154:975-81.
 20. Hagen PJ, Hartmann IJ, Hoekstra OS, et al. How to use a gestalt interpretation for ventilation-perfusion lung scintigraphy. *J Nucl Med* 2002;43:1317-23.
 21. Sostman HD, Miniati M, Gottschalk A, et al. Sensitivity and specificity of perfusion scintigraphy combined with chest radiography for acute pulmonary embolism in PIOPED II. *J Nucl Med* 2008;49:1741-8.
 22. Cronin P, Dwamena BA. A clinically meaningful interpretation of the Prospective Investigation of Pulmonary Embolism Diagnosis (PIOPED) Scintigraphic Data. *Acad Radiol* 2017;24:550-62.
 23. Reinartz P, Wildberger JE, Schaefer W, et al. Tomographic imaging in the diagnosis of pulmonary embolism: a comparison between V/Q lung scintigraphy in SPECT technique and multislice spiral CT. *J Nucl Med* 2004;45:1501-8.
 24. Gottschalk A, Stein PD, Goodman LR, et al. Overview of Prospective Investigation of Pulmonary Embolism Diagnosis II. *Semin Nucl Med* 2002;32:173-82.
 25. Stein PD, Fowler SE, Goodman LR, et al. Multidetector computed tomography for acute pulmonary embolism. *N Engl J Med* 2006;354:2317-27.
 26. Berdahl CT, Vermeulen MJ, Larson DB, et al. Emergency department computed tomography utilization in the United States and Canada. *Ann Emerg Med* 2013;62:486-94. e3.
 27. White CS, Kuo D, Kelemen M, et al. Chest pain evaluation in the emergency department: can MDCT provide a comprehensive evaluation? *AJR Am J Roentgenol* 2005;185:533-40.
 28. Woo JK, Chiu RY, Thakur Y, et al. Risk-benefit analysis of pulmonary CT angiography in patients with suspected pulmonary embolus. *AJR Am J Roentgenol* 2012;198:1332-9.
 29. Luk L, Steinman J, Newhouse JH. Intravenous Contrast-Induced Nephropathy-The Rise and Fall of a Threatening Idea. *Adv Chronic Kidney Dis* 2017;24:169-75.
 30. Heller M, Krieger P, Finefrock D, et al. Contrast CT Scans in the Emergency Department Do Not Increase Risk of Adverse Renal Outcomes. *West J Emerg Med* 2016;17:404-8.
 31. Beckett KR, Moriarity AK, Langer JM. Safe Use of Contrast Media: What the Radiologist Needs to Know. *Radiographics* 2015;35:1738-50.
 32. Katayama H, Yamaguchi K, Kozuka T, et al. Adverse reactions to ionic and nonionic contrast media. A report from the Japanese Committee on the Safety of Contrast Media. *Radiology* 1990;175:621-8.
 33. Li X, Chen J, Zhang L, et al. Clinical observation of the adverse drug reactions caused by non-ionic iodinated contrast media: results from 109,255 cases who underwent enhanced CT examination in Chongqing, China. *Br J Radiol* 2015;88:20140491.

34. Wittram C. How I do it: CT pulmonary angiography. *AJR Am J Roentgenol* 2007;188:1255-61.
35. Palacio D, Benveniste MF, Betancourt-Cuellar SL, et al. Multidetector computed tomography pulmonary angiography pitfalls in the evaluation of pulmonary embolism with emphasis in technique. *Semin Roentgenol* 2015;50:217-25.
36. Chen YH, Velayudhan V, Weltman DI, et al. Waiting to exhale: salvaging the nondiagnostic CT pulmonary angiogram by using expiratory imaging to improve contrast dynamics. *Emerg Radiol* 2008;15:161-9.
37. Kuzo RS, Pooley RA, Crook JE, et al. Measurement of caval blood flow with MRI during respiratory maneuvers: implications for vascular contrast opacification on pulmonary CT angiographic studies. *AJR Am J Roentgenol* 2007;188:839-42.
38. Mortimer AM, Singh RK, Hughes J, et al. Use of expiratory CT pulmonary angiography to reduce inspiration and breath-hold associated artefact: contrast dynamics and implications for scan protocol. *Clin Radiol* 2011;66:1159-66.
39. Marten K, Engelke C, Funke M, et al. ECG-gated Multislice Spiral CT for diagnosis of acute pulmonary embolism. *Clinical Radiology* 2003;58:862-8.
40. Ghaye B, Remy J, Remy-Jardin M. Non-traumatic thoracic emergencies: CT diagnosis of acute pulmonary embolism: the first 10 years. *Eur Radiol* 2002;12:1886-905.
41. Remy-Jardin M, Remy J, Wattinne L, et al. Central pulmonary thromboembolism: diagnosis with spiral volumetric CT with the single-breath-hold technique-comparison with pulmonary angiography. *Radiology* 1992;185:381-7.
42. Shah AA, Davis SD, Gamsu G, et al. Parenchymal and pleural findings in patients with and patients without acute pulmonary embolism detected at spiral CT. *Radiology* 1999;211:147-53.
43. Schwickert HC, Schweden F, Schild HH, et al. Pulmonary arteries and lung parenchyma in chronic pulmonary embolism: preoperative and postoperative CT findings. *Radiology* 1994;191:351-7.
44. Im DJ, Hur J, Han KH, et al. Acute pulmonary embolism: retrospective cohort study of the predictive value of perfusion defect volume measured with dual-energy CT. *AJR Am J Roentgenol* 2017;209:1015-22.
45. Apfaltrer P, Walter T, Gruettner J, et al. Prediction of adverse clinical outcome in patients with acute pulmonary embolism: evaluation of high-sensitivity troponin I and quantitative CT parameters. *Eur J Radiol* 2013;82:563-7.
46. Kang DK, Thilo C, Schoepf UJ, et al. CT signs of right ventricular dysfunction: prognostic role in acute pulmonary embolism. *JACC Cardiovasc Imaging* 2011;4:841-9.
47. Mastora I, Remy-Jardin M, Masson P, et al. Severity of acute pulmonary embolism: evaluation of a new spiral CT angiographic score in correlation with echocardiographic data. *Eur Radiol* 2003;13:29-35.
48. Qanadli SD, El Hajjam M, Vieillard-Baron A, et al. New CT index to quantify arterial obstruction in pulmonary embolism: comparison with angiographic index and echocardiography. *AJR Am J Roentgenol* 2001;176:1415-20.
49. Kubo T, Lin PJ, Stiller W, et al. Radiation dose reduction in chest CT: a review. *AJR Am J Roentgenol* 2008;190:335-43.
50. Mayo J, Thakur Y. Pulmonary CT angiography as first-line imaging for PE: image quality and radiation dose considerations. *AJR Am J Roentgenol* 2013;200:522-8.
51. Ridge CA, Litmanovich D, Bukoye BA, et al. Computed tomography angiography for suspected pulmonary embolism: comparison of 2 adaptive statistical iterative reconstruction blends to filtered back-projection alone. *J Comput Assist Tomogr* 2013;37:712-7.
52. Pontana F, Henry S, Duhamel A, et al. Impact of iterative reconstruction on the diagnosis of acute pulmonary embolism (PE) on reduced-dose chest CT angiograms. *Eur Radiol* 2015;25:1182-9.
53. Cho ES, Chung JJ, Kim S, et al. CT venography for deep vein thrombosis using a low tube voltage (100 kVp) setting could increase venous enhancement and reduce the amount of administered iodine. *Korean J Radiol* 2013;14:183-93.
54. Bogot NR, Fingerle A, Shaham D, et al. Image quality of low-energy pulmonary CT angiography: comparison with standard CT. *AJR Am J Roentgenol* 2011;197:W273-8.
55. Schueller-Weidekamm C, Schaefer-Prokop CM, Weber M, et al. CT angiography of pulmonary arteries to detect pulmonary embolism: improvement of vascular enhancement with low kilovoltage settings. *Radiology* 2006;241:899-907.
56. Petersilka M, Bruder H, Krauss B, et al. Technical principles of dual source CT. *Eur J Radiol* 2008;68:362-8.
57. Kerl JM, Lehnert T, Schell B, et al. Intravenous contrast material administration at high-pitch dual-source CT pulmonary angiography: test bolus versus bolus-tracking technique. *Eur J Radiol* 2012;81:2887-91.
58. Bauer RW, Schell B, Beeres M, et al. High-pitch dual-source computed tomography pulmonary angiography in freely breathing patients. *J Thorac Imaging* 2012;27:376-81.
59. Hou DJ, Tso DK, Davison C, et al. Clinical utility of

- ultra high pitch dual source thoracic CT imaging of acute pulmonary embolism in the emergency department: are we one step closer towards a non-gated triple rule out? *Eur J Radiol* 2013;82:1793-8.
60. Bucher AM, Kerl MJ, Albrecht MH, et al. Systematic comparison of reduced tube current protocols for high-pitch and standard-pitch pulmonary CT angiography in a large single-center population. *Acad Radiol* 2016;23:619-27.
 61. Lu GM, Luo S, Meinel FG, et al. High-pitch computed tomography pulmonary angiography with iterative reconstruction at 80 kVp and 20 mL contrast agent volume. *Eur Radiol* 2014;24:3260-8.
 62. Martini K, Meier A, Higashigaito K, et al. Prospective randomized comparison of high-pitch CT at 80 kVp under free breathing with standard-pitch CT at 100 kVp under breath-hold for detection of pulmonary embolism. *Acad Radiol* 2016;23:1335-41.
 63. Meinel FG, Canstein C, Schoepf UJ, et al. Image quality and radiation dose of low tube voltage 3rd generation dual-source coronary CT angiography in obese patients: a phantom study. *Eur Radiol* 2014;24:1643-50.
 64. Saade C, Mayat A, El-Merhi F. Exponentially decelerated contrast media injection rate combined with a novel patient-specific contrast formula reduces contrast volume administration and radiation dose during computed tomography pulmonary angiography. *J Comput Assist Tomogr* 2016;40:370-4.
 65. Ohana M, Jeung MY, Labani A, et al. Thoracic dual energy CT: acquisition protocols, current applications and future developments. *Diagn Interv Imaging* 2014;95:1017-26.
 66. Johnson TR. Dual-energy CT: general principles. *AJR Am J Roentgenol* 2012;199:S3-8.
 67. Danad I, Fayad ZA, Willeminck MJ, et al. New Applications of Cardiac Computed Tomography: Dual-Energy, Spectral, and Molecular CT Imaging. *JACC Cardiovasc Imaging* 2015;8:710-23.
 68. Rassouli N, Etesami M, Dhanantwari A, et al. Detector-based spectral CT with a novel dual-layer technology: principles and applications. *Insights Imaging* 2017;8:589-98.
 69. Lu GM, Zhao Y, Zhang LJ, et al. Dual-energy CT of the lung. *AJR Am J Roentgenol* 2012;199:S40-53.
 70. Thieme SF, Becker CR, Hacker M, et al. Dual energy CT for the assessment of lung perfusion--correlation to scintigraphy. *Eur J Radiol* 2008;68:369-74.
 71. Okada M, Kunihiro Y, Nakashima Y, et al. Added value of lung perfused blood volume images using dual-energy CT for assessment of acute pulmonary embolism. *Eur J Radiol* 2015;84:172-7.
 72. Dournes G, Verdier D, Montaudon M, et al. Dual-energy CT perfusion and angiography in chronic thromboembolic pulmonary hypertension: diagnostic accuracy and concordance with radionuclide scintigraphy. *Eur Radiol* 2014;24:42-51.
 73. Chae EJ, Seo JB, Jang YM, et al. Dual-energy CT for assessment of the severity of acute pulmonary embolism: pulmonary perfusion defect score compared with CT angiographic obstruction score and right ventricular/left ventricular diameter ratio. *AJR Am J Roentgenol* 2010;194:604-10.
 74. Apfaltrer P, Bachmann V, Meyer M, et al. Prognostic value of perfusion defect volume at dual energy CTA in patients with pulmonary embolism: correlation with CTA obstruction scores, CT parameters of right ventricular dysfunction and adverse clinical outcome. *Eur J Radiol* 2012;81:3592-7.
 75. Meinel FG, Graef A, Bamberg F, et al. Effectiveness of automated quantification of pulmonary perfused blood volume using dual-energy CTPA for the severity assessment of acute pulmonary embolism. *Invest Radiol* 2013;48:563-9.
 76. Apfaltrer P, Sudarski S, Schneider D, et al. Value of monoenergetic low-kV dual energy CT datasets for improved image quality of CT pulmonary angiography. *Eur J Radiol* 2014;83:322-8.
 77. Delesalle MA, Pontana F, Duhamel A, et al. Spectral optimization of chest CT angiography with reduced iodine load: experience in 80 patients evaluated with dual-source, dual-energy CT. *Radiology* 2013;267:256-66.
 78. Yuan R, Shuman WP, Earls JP, et al. Reduced iodine load at CT pulmonary angiography with dual-energy monochromatic imaging: comparison with standard CT pulmonary angiography--a prospective randomized trial. *Radiology* 2012;262:290-7.
 79. Johnson SA, Stevens SM, Woller SC, et al. Risk of deep vein thrombosis following a single negative whole-leg compression ultrasound: a systematic review and meta-analysis. *JAMA* 2010;303:438-45.
 80. Goodacre S, Sampson F, Thomas S, et al. Systematic review and meta-analysis of the diagnostic accuracy of ultrasonography for deep vein thrombosis. *BMC Med Imaging* 2005;5:6.
 81. Bates SM, Jaeschke R, Stevens SM, et al. Diagnosis of DVT: Antithrombotic Therapy and Prevention of Thrombosis, 9th ed: American College of Chest Physicians Evidence-Based Clinical Practice Guidelines. *Chest* 2012;141:e351S-418S.

82. Guanella R, Righini M. Serial limited versus single complete compression ultrasonography for the diagnosis of lower extremity deep vein thrombosis. *Semin Respir Crit Care Med* 2012;33:144-50.
83. Bernardi E, Camporese G, Buller HR, et al. Serial 2-point ultrasonography plus D-dimer vs whole-leg color-coded Doppler ultrasonography for diagnosing suspected symptomatic deep vein thrombosis: a randomized controlled trial. *JAMA* 2008;300:1653-9.
84. Loud PA, Katz DS, Belfi L, et al. Imaging of deep venous thrombosis in suspected pulmonary embolism. *Semin Roentgenol* 2005;40:33-40.
85. Ghaye B, Dondelinger RF. Non-traumatic thoracic emergencies: CT venography in an integrated diagnostic strategy of acute pulmonary embolism and venous thrombosis. *Eur Radiol* 2002;12:1906-21.
86. Reichert M, Henzler T, Krissak R, et al. Venous thromboembolism: additional diagnostic value and radiation dose of pelvic CT venography in patients with suspected pulmonary embolism. *Eur J Radiol* 2011;80:50-3.
87. Stein PD, Woodard PK, Weg JG, et al. Diagnostic pathways in acute pulmonary embolism: recommendations of the PIOPED II Investigators. *Radiology* 2007;242:15-21.
88. Goodman LR, Stein PD, Matta F, et al. CT venography and compression sonography are diagnostically equivalent: data from PIOPED II. *AJR Am J Roentgenol* 2007;189:1071-6.
89. Garcia-Bolado A, Del Cura JL. CT venography vs ultrasound in the diagnosis of thromboembolic disease in patients with clinical suspicion of pulmonary embolism. *Emerg Radiol* 2007;14:403-9.
90. Shi WY, Wang LW, Wang SJ, et al. Combined direct and indirect CT Venography (Combined CTV) in detecting lower extremity deep vein thrombosis. *Medicine (Baltimore)* 2016;95:e3010.
91. Duwe KM, Shiau M, Budorick NE, et al. Evaluation of the lower extremity veins in patients with suspected pulmonary embolism: a retrospective comparison of helical CT venography and sonography. 2000 ARRS Executive Council Award I. American Roentgen Ray Society. *AJR Am J Roentgenol* 2000;175:1525-31.
92. Johnson JC, Brown MD, McCullough N, et al. CT lower extremity venography in suspected pulmonary embolism in the ED. *Emerg Radiol* 2006;12:160-3.
93. Hochegger B, Ley-Zaporozhan J, Marchiori E, et al. Magnetic resonance imaging findings in acute pulmonary embolism. *Br J Radiol* 2011;84:282-7.
94. Kluge A, Luboldt W, Bachmann G. Acute pulmonary embolism to the subsegmental level: diagnostic accuracy of three MRI techniques compared with 16-MDCT. *AJR Am J Roentgenol* 2006;187:W7-14.
95. Ley S, Grunig E, Kiely DG, et al. Computed tomography and magnetic resonance imaging of pulmonary hypertension: Pulmonary vessels and right ventricle. *J Magn Reson Imaging* 2010;32:1313-24.
96. Kreitner KF, Kunz RP, Ley S, et al. Chronic thromboembolic pulmonary hypertension - assessment by magnetic resonance imaging. *Eur Radiol* 2007;17:11-21.
97. Kalb B, Sharma P, Tigges S, et al. MR imaging of pulmonary embolism: diagnostic accuracy of contrast-enhanced 3D MR pulmonary angiography, contrast-enhanced low-flip angle 3D GRE, and nonenhanced free-induction FISP sequences. *Radiology* 2012;263:271-8.
98. Huisman MV, Klok FA. Magnetic resonance imaging for diagnosis of acute pulmonary embolism: not yet a suitable alternative to CT-PA. *J Thromb Haemost* 2012;10:741-2.
99. Stein PD, Chenevert TL, Fowler SE, et al. Gadolinium-enhanced magnetic resonance angiography for pulmonary embolism: a multicenter prospective study (PIOPED III). *Ann Intern Med* 2010;152:434-43, W142-3.
100. Expert Panels on Cardiac and Thoracic Imaging, Kirsch J, Brown RKJ, et al. ACR Appropriateness Criteria(R) Acute Chest Pain-Suspected Pulmonary Embolism. *J Am Coll Radiol* 2017;14:S2-12.
101. Reiter U, Reiter G, Fuchsjager M. MR phase-contrast imaging in pulmonary hypertension. *Br J Radiol* 2016;89:20150995.
102. Grothues F, Moon JC, Bellenger NG, et al. Interstudy reproducibility of right ventricular volumes, function, and mass with cardiovascular magnetic resonance. *Am Heart J* 2004;147:218-23.
103. Raja AS, Greenberg JO, Qaseem A, et al. Evaluation of Patients With Suspected Acute Pulmonary Embolism: Best Practice Advice From the Clinical Guidelines Committee of the American College of Physicians. *Ann Intern Med* 2015;163:701-11.
104. Grifoni S, Olivotto I, Cecchini P, et al. Short-term clinical outcome of patients with acute pulmonary embolism, normal blood pressure, and echocardiographic right ventricular dysfunction. *Circulation* 2000;101:2817-22.
105. Ribeiro A, Lindmarker P, Juhlin-Dannfelt A, et al. Echocardiography Doppler in pulmonary embolism: right ventricular dysfunction as a predictor of mortality rate. *Am Heart J* 1997;134:479-87.
106. Lang RM, Badano LP, Mor-Avi V, et al. Recommendations for cardiac chamber quantification by echocardiography

- in adults: an update from the American Society of Echocardiography and the European Association of Cardiovascular Imaging. *J Am Soc Echocardiogr* 2015;28:1-39. e14.
107. Grifoni S, Olivotto I, Cecchini P, et al. Utility of an integrated clinical, echocardiographic, and venous ultrasonographic approach for triage of patients with suspected pulmonary embolism. *Am J Cardiol* 1998;82:1230-5.
 108. McConnell MV, Solomon SD, Rayan ME, et al. Regional right ventricular dysfunction detected by echocardiography in acute pulmonary embolism. *Am J Cardiol* 1996;78:469-73.
 109. Kurzyna M, Torbicki A, Pruszczyk P, et al. Disturbed right ventricular ejection pattern as a new Doppler echocardiographic sign of acute pulmonary embolism. *Am J Cardiol* 2002;90:507-11.
 110. Pruszczyk P, Torbicki A, Kuch-Wocjal A, et al. Diagnostic value of transoesophageal echocardiography in suspected haemodynamically significant pulmonary embolism. *Heart* 2001;85:628-34.
 111. Comess KA, DeRook FA, Russell ML, et al. The incidence of pulmonary embolism in unexplained sudden cardiac arrest with pulseless electrical activity. *Am J Med* 2000;109:351-6.
 112. Investigators P. Value of the ventilation/perfusion scan in acute pulmonary embolism. Results of the prospective investigation of pulmonary embolism diagnosis (PIOPED). *JAMA* 1990;263:2753-9.
 113. Walsh PN, Greenspan RH, Simon M, et al. Angiographic Severity Index for Pulmonary-Embolism. *Circulation* 1973;47:101-8.
 114. Miller GA, Sutton GC, Kerr IH, et al. Comparison of streptokinase and heparin in treatment of isolated acute massive pulmonary embolism. *Br Med J* 1971;2:681-4.
 115. Wittram C, Waltman AC, Shepard JA, et al. Discordance between CT and angiography in the PIOPED II study. *Radiology* 2007;244:883-9.
 116. Stein PD, Henry JW, Gottschalk A. Reassessment of pulmonary angiography for the diagnosis of pulmonary embolism: relation of interpreter agreement to the order of the involved pulmonary arterial branch. *Radiology* 1999;210:689-91.
 117. Hofmann LV, Lee DS, Gupta A, et al. Safety and hemodynamic effects of pulmonary angiography in patients with pulmonary hypertension: 10-year single-center experience. *AJR Am J Roentgenol* 2004;183:779-86.
 118. Mills SR, Jackson DC, Older RA, et al. The incidence, etiologies, and avoidance of complications of pulmonary angiography in a large series. *Radiology* 1980;136:295-9.
 119. Di Nisio M, van Es N, Buller HR. Deep vein thrombosis and pulmonary embolism. *Lancet* 2016;388:3060-73.
 120. Schembri GP, Miller AE, Smart R. Radiation dosimetry and safety issues in the investigation of pulmonary embolism. *Semin Nucl Med* 2010;40:442-54.

Cite this article as: Moore AJ, Wachsmann J, Chamarthy MR, Panjikanan L, Tanabe Y, Rajiah P. Imaging of acute pulmonary embolism: an update. *Cardiovasc Diagn Ther* 2018;8(3):225-243. doi: 10.21037/cdt.2017.12.01